ACS central science

http://pubs.acs.org/journal/acscii

Research Article

Precisely Structured Nitric-Oxide-Releasing Copolymer Brush Defeats Broad-Spectrum Catheter-Associated Biofilm Infections *In Vivo*

Zheng Hou, Yang Wu, Chen Xu, Sheethal Reghu, Zifang Shang, Jingjie Chen, Dicky Pranantyo, Kalisvar Marimuth, Partha Pratim De, Oon Tek Ng, Kevin Pethe, En-Tang Kang, Peng Li,* and Mary B. Chan-Park*

Cite This: *ACS Cent. Sci.* 2020, 6, 2031−2045

Read Online

ACCESS | Metrics & More | Article Recommendations | Supporting Information

ABSTRACT: Gram-negative bacteria cannot be easily eradicated by antibiotics and are a major source of recalcitrant infections of indwelling medical devices. Among various device-associated infections, intravascular catheter infection is a leading cause of mortality. Prior approaches to surface modification, such as antibiotics impregnation, hydrophilization, unstructured NO-releasing, etc., have failed to achieve adequate infection-resistant coatings. We report a precision-structured diblock copolymer brush (H(N)-*b*-S) composed of a surface antifouling block of poly(sulfobetaine methacrylate) (S) and a subsurface bactericidal block (H(N)) of nitric-oxide-emitting functionalized poly(hydroxyethyl methacrylate) (H) covalently grafted from the inner and outer surfaces of a polyurethane catheter. The block copolymer architecture of the coating is important for achieving good broad-spectrum anti-biofilm activity with good biocompatibility and low fouling. The coating procedure is scalable to clinically useful catheter lengths. Only the block copolymer brush coating ((H(N)-*b*-S)) shows unprecedented, above 99.99%, in vitro biofilm inhibition of Gram-positive and Gram-negative bacteria, 100-fold better than previous coatings. It has negligible toxicity toward mammalian cells and excellent blood compatibility. In a murine subcutaneous infection model, it achieves >99.99% biofilm reduction of Gram-positive and Gram-negative bacteria compared with <90% for silver catheter, while in a porcine central venous catheter infection model, it achieves >99.99% reduction of MRSA with 5-day implantation. This precision coating is readily applicable for long-term biofilm-resistant and blood-compatible copolymer coatings covalently grafted from a wide range of medical devices.

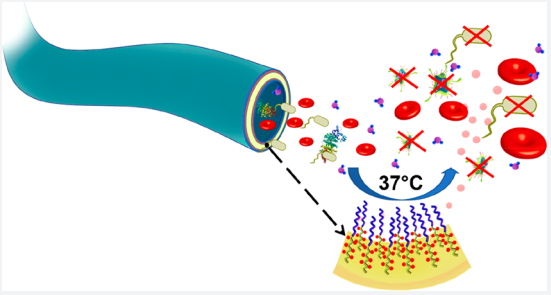

1. INTRODUCTION

Medical implants are ubiquitous modern interventions that ameliorate suffering and provide convenience and comfort but are also a major source of infections. Bacteria from patients' microflora can attach to foreign implants even with the most sterile methods and develop into biofilm form that is recalcitrant to antibiotics treatment. Device-associated infections (DAIs) are a major unsolved healthcare problem that leads to significant morbidity and mortality and large economic costs. Reduction of DAIs through anti-infective surface modification of devices is challenging due to the broad spectrum of bacteria whose colonization and proliferation on device surfaces must be suppressed. Particularly difficult to suppress are Gram-negative bacteria that are intrinsically resistant to many antibiotics.[1−3] At present, there is no biofilm-resistant coating for major indwelling devices such as catheters and ventilators[4,5] that can effectively prevent device-associated infections in clinical settings.[6]

Catheters are relatively simple medical devices that are ubiquitous in clinical settings and that frequently become infected; some of these infections, such as central line associated bloodstream infections, can be very dangerous.[7] As such, they provide a useful test-bed for development and application of anti-infective device surface modifications. The small and long bores of typical catheters make their inner surfaces not easily uniformly modifiable by common techniques.[8] An ideal biofilm-resistant coating should be broad-spectrum antifouling on the device surface to reduce bacterial contamination there but also broad-spectrum antibacterial in order to kill any bacteria that do attach to the device surface. Moreover, the coated medical device should be nontoxic and nonthrombogenic. The biofilm inhibition effects ideally should persist for as long as the device is

Received: June 8, 2020
Published: October 29, 2020

https://dx.doi.org/10.1021/acscentsci.0c00755
ACS Cent. Sci. 2020, 6, 2031−2045

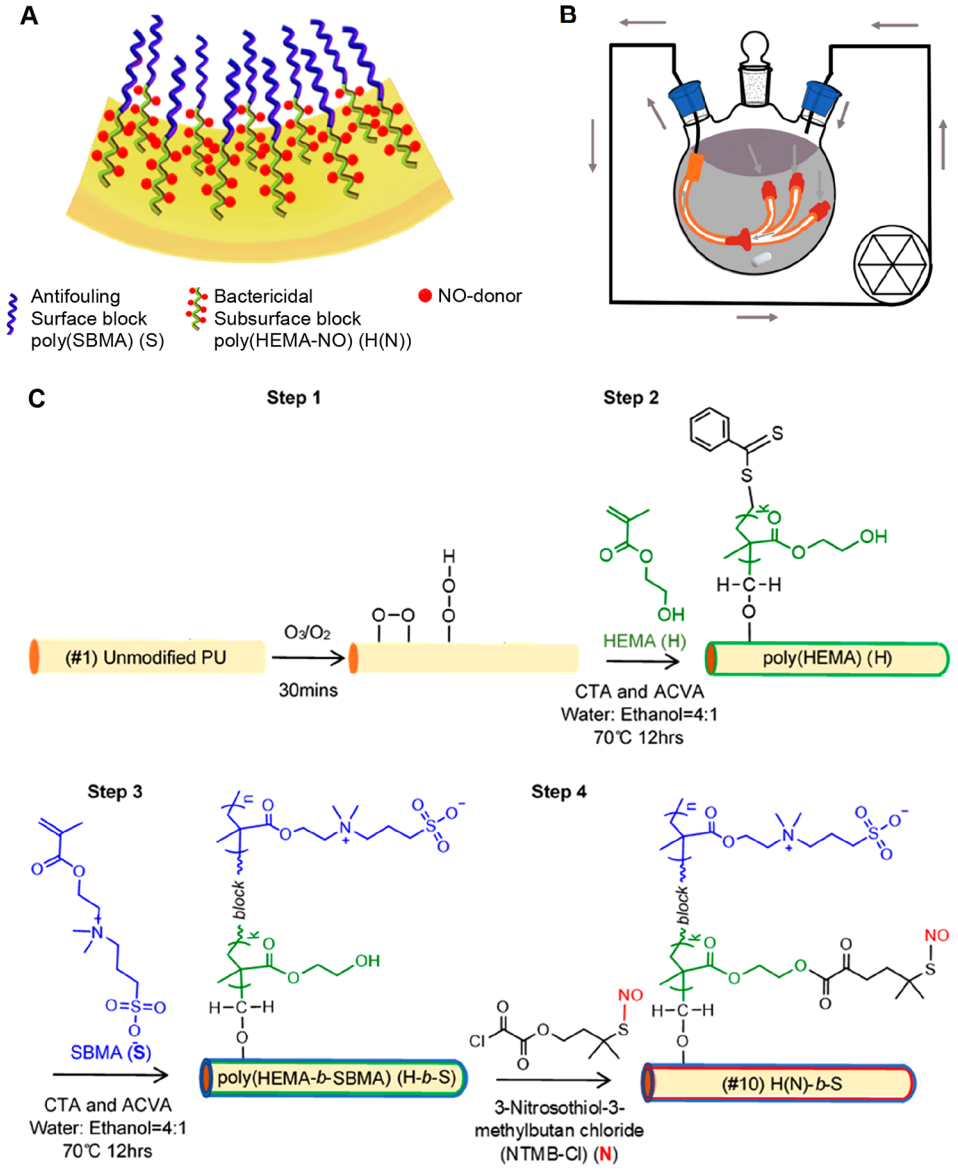

Figure 1. Illustrations and synthesis scheme of antifouling and nitric oxide (NO) emitting diblock copolymer brush ((#10) H(N)-*b*-S) grafted from a PU catheter: (A) The diblock copolymer with a subsurface NO-emitting block modified from poly(HEMA) (H) with a RSNO (N) and a surface block of antifouling poly(SBMA) (S). (B) Flow reactor for surface modification of a long catheter with long narrow lumen (gray arrows: flow of monomer solution). (C) Synthesis scheme of diblock copolymer (#10) H(N)-*b*-S coating via ozone pretreatment of PU followed by surface-initiated RAFT diblock copolymerization. (CTA is chain transfer agent of 4-cyano-4-(phenylcarbonothioylthio) pentanoic acid (CPCPA), and ACVA is the thermal initiator 4,4′-azobis(4-cyanopentanoic acid)).

implanted. To prevent leaching or solvation of the coating materials or antimicrobial agents into the bloodstream or body fluids and for long-term stability, covalent grafting as opposed to physical adsorption of the coating onto the surface is preferable.[9,10] Thus far, there is no report of an effective biofilm-resistant coating that can meet the above multifaceted requirements for clinically useful (30 cm or more) catheter lengths.

Various strategies for biofilm-resistant catheter modifications have been investigated.[5] Among these, antifouling coatings made from purely hydrophilic polymers such as the zwitterionic poly(sulfobetaine methacrylate) (poly(SBMA))[11] prevent bacteria adhesion but have no antibacterial efficacy so that their long-term antibiofilm effect is usually modest (less than 2.0$\log_{10}$ (99%) inhibition).[12−14] Silver coatings have been tested *in vivo*, but their biofilm inhibition efficacies are generally poor.[5,15] Antibiotics are ineffective against many biofilm bacteria,[5,16,17] and current clinical guidelines do not recommend prolonged elution of antibiotics into the body from implanted devices due to the rapid emergence of antimicrobial resistance.[1]

Sustained release of a bactericidal transient gas may satisfy the requirement for a long-term antibiofilm coating that does not cause device fouling and toxicity.[18] Nitric oxide (NO) gas is an endogenous molecule that is both antibacterial and antithrombogenic. NO has a short (subsecond) biological half-life and a small (around 100 μm) diffusion radius as it is rapidly quenched by molecular oxygen or biomolecules (e.g., oxyhemoglobin).[19,20] Because of its short half-life, NO exploited for antibiofilm device coating must be generated and released *in situ*.[21] However, NO-donors are usually toxic. NO-donors employed in anti-infective device coatings are

https://dx.doi.org/10.1021/acscentsci.0c00755
ACS Cent. Sci. 2020, 6, 2031−2045

Table 1. Summary of Coating Polymers on Polyurethane Catheter

coating no.	label	coating polymer	method of synthesis	synthetic scheme
1	unmodified	none	uncoated	
2	silver	commercial silver coated catheter	purchased	
3	S	homo poly(SBMA)	free radical polymerization of SBMA	Figure S1A
4	H(N)	homo poly(HEMA-NO)	free radical polymerization of HEMA and then reaction with NO-donor (NTMB-Cl)	Figure S1B
5	H-*x*-S	cross-linked hydrogel of poly(SBMA-*co*-HEMA)	free radical copolymerization of SBMA, HEMA with cross-linker	Figure S2
6	H-*r*-S	poly(HEMA-*ran*-SBMA)	free radical copolymerization of SBMA and HEMA	Figure S3
7	H-*b*-S	poly(HEMA-*block*-SBMA)	RAFT block copolymerization of HEMA followed by SBMA	Figure 1C
8	H(N)-*x*-S	cross-linked hydrogel of poly(SBMA-*co*-HEMA(NO))	free radical copolymerization of SBMA, HEMA with cross-linker and then reaction with NTMB-Cl	Figure S2
9	H(N)-*r*-S	poly((HEMA-NO)-*ran*-SBMA)	free radical copolymerization of SBMA and HEMA and then reaction with NTMB-Cl	Figure S3
10	H(N)-*b*-S (optimum)	poly((HEMA-NO)-*block*-SBMA))	RAFT block copolymerization of HEMA followed by SBMA then reaction with NTMB-Cl	Figure 1C

usually blended with the coating material and are leachable, which results in toxicity.[22−24] Thus far, there is no report of covalent immobilization of NO-donor with precise spatial control of the donor depth within a hydrophilic coating. Further, these long-last donors (typically *S*-nitrosothiols (RSNO)) are usually hydrophobic so that their presence would promote surface fouling by blood proteins and bacteria. What is needed is a precision-structured coating that incorporates immobilized NO-donors deeper into the coating rather than at the surface, thereby exploiting the desirable property of NO gas emission while avoiding the fouling side effects of NO-donors themselves at the coating surface.

Herein, we report a novel uniform high-density precision diblock copolymer brush (termed H(N)-*b*-S) consisting of a surface block of antifouling poly(sulfobetaine methacrylate) (labeled as S) with a subsurface block of bactericidal RSNO-modified poly(hydroxyethyl methacrylate) (labeled as H(N)) (Figure 1A). This material is covalently "grafted from" a slender polyurethane (PU) catheter and shows outstanding broad spectrum antibiofilm efficacy *in vitro* and *in vivo*. The brush also has good antithrombogenicity and biocompatibility. We designed a flow reactor (Figure 1B) to scale up the H(N)-*b*-S coating procedure to modify a 30 cm long catheter.

2. RESULTS

2.1. Surface Modification Chemistries. To evaluate the importance of the precision diblock copolymer structure, two controls which are (#1) uncoated catheter and (#2) silver-coated catheter, and eight polymer coatings with different architectures (#3 to #10) made using the same monomers (hydroxyethyl methacrylate (HEMA) and sulfobetaine methacrylate (SBMA)) were tested (Table 1). The H(N)-*b*-S (#10, Table 1) coated catheters showed the most optimal effectiveness to reduce biofilm-related infections due to a range of Gram-positive and Gram-negative bacteria.

To covalently graft the precision diblock copolymer (#10) H(N)-*b*-S from both the inner and outer surfaces of a slender polyurethane (PU) catheter, we invented a new catheter surface modification method of ozone-initiated surface reversible addition−fragmentation chain-transfer (ozone-surface-RAFT) block copolymerization (Figure 1C). The PU surface is activated by ozone to create a high areal density of peroxide/hydroperoxide initiators. Then, the inner (subsurface) block of poly(HEMA) (H) is "grafted from" the surface initiators by polymerizing HEMA monomer in the presence of a chain transfer agent (CTA) and a thermal initiator (4,4′-azobis(4-cyanovaleric acid), ACVA).[25,26] A subsequent RAFT-mediated block copolymerization of SBMA is then performed to produce the contiguous outer (surface) block (S).[27] The resultant H-*b*-S diblock brush (coating #7, Table 1) is then postmodified by reacting the constituent H block with an RSNO which functions as a NO-donor (denoted as N) to produce the NO-emitting precision structured (#10) H(N)-*b*-S diblock brush (Figure 1C). The RSNO employed is 3-nitrosothiol-3-methylbutan-chloride (NTMB-Cl).

We also investigated homopolymer brushes (#3) S and (#4) H(N) (Table 1) composed of homo poly(SBMA) and RSNO-functionalized poly(HEMA) respectively made via surface-initiated free radical polymerization (Figure S1). Further, we investigated the cross-linked hydrogel coating ((#5) H-*x*-S) and random copolymer brush ((#6) H-*r*-S) (Table 1) made from the two monomers (HEMA and SBMA) via free radical copolymerization (Figures S2 and S3). (Coating #7 is the H-*b*-S diblock made via ozone-surface-RAFT block copolymerization as described above.) Using the (#5)−(#7) coatings, the HEMA component was further postmodified by reacting with the RSNO-donor (denoted "N"), specifically 3-nitrosothiol-3-methylbutan-chloride (NTMB-Cl), to produce the respective NO-emitting counterpart coatings (#8) to (#10) (Table 1, Figures 1C, S2 and S3).

2.2. Surface Characterization. Figure 2A(i) shows the gross visual appearance of a pristine 30 cm long PU catheter control to be transparent and almost colorless. After coating with (#10) H(N)-*b*-S (Figure 2A(ii)), the catheter color changes to a homogeneous dark green, which is due to the presence of the tertiary nitrosothiol group in NTMB. Fourier transform infrared with attenuated total reflection (FTIR-ATR) spectroscopy was employed to verify the successful surface block copolymerization of (#10) H(N)-*b*-S. Compared with the unmodified PU control (Figure 2B(i)), the first block, poly(HEMA) (Figure 2B(ii)), exhibited an increased peak intensity at 1742 cm^{-1} and the appearance of a new peak at 1020 cm^{-1}, corroborating the addition of the ester carbonyl group (C═O) and hydroxyl (C−O−H) group due to HEMA. The success of the second block copolymerization step to form the contiguous poly(SBMA) block of (#7) (H-*b*-S) was proven by the appearance of the sulfonyl signal at 1040 cm^{-1} (Figure 2B(iii)); however, the C−O−H group signal (1020 cm^{-1}) from the underlying poly(HEMA) block (H) was still detectable. In the spectrum of (#10) H(N)-*b*-S (Figure

https://dx.doi.org/10.1021/acscentsci.0c00755
ACS Cent. Sci. 2020, 6, 2031−2045

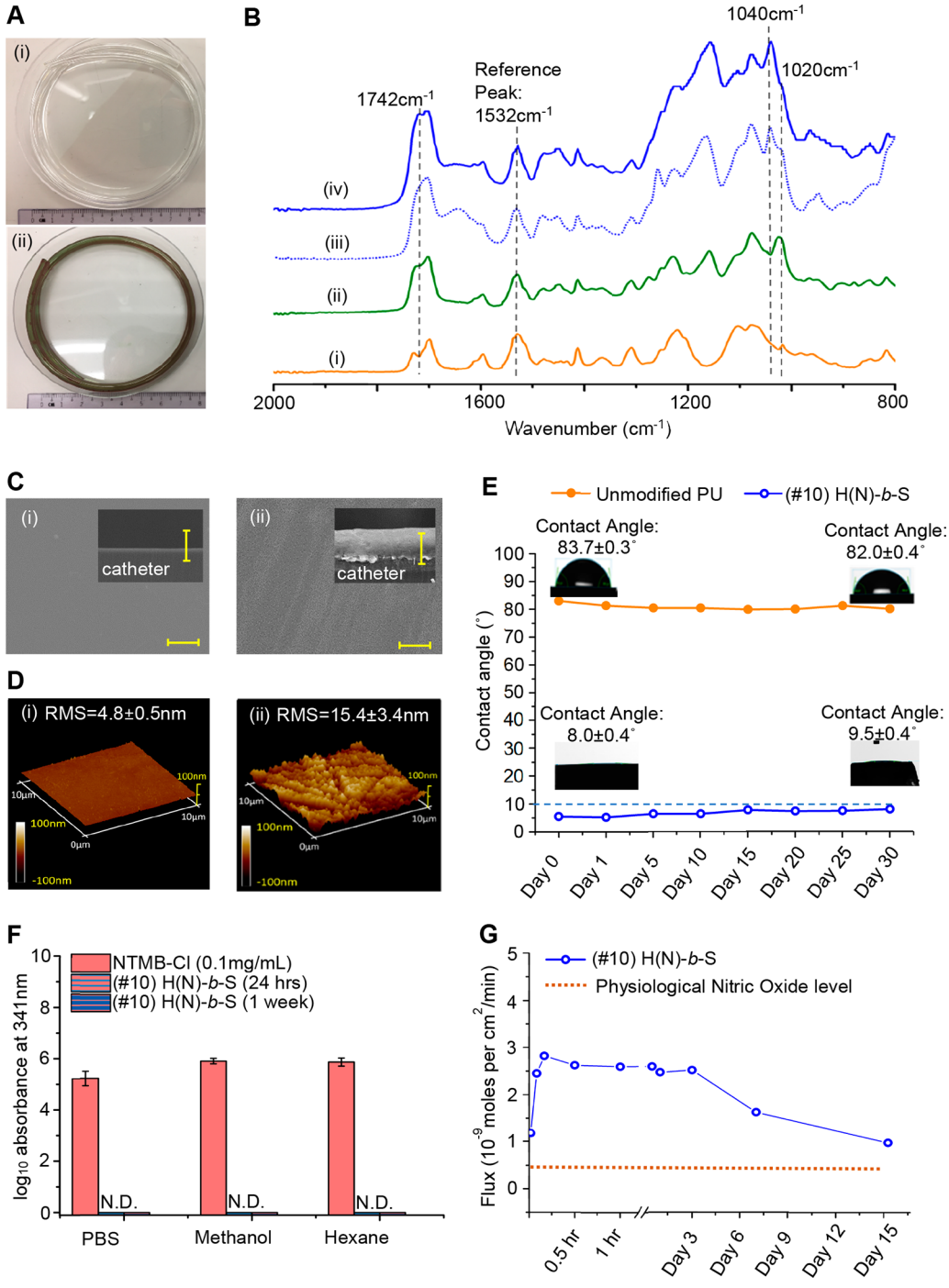

Figure 2. Characterization of (#10) H(N)-*b*-S coating: (A) Visual appearance of long (i) (#1) unmodified and (ii) (#10) H(N)-*b*-S coated catheters. (B) FTIR-ATR characterization of steps in the synthesis of (#10) block copolymer coating: (i) unmodified PU control, (ii) first block of poly(HEMA), (iii) after second block copolymerization to make (#7) H-*b*-S, (iv) reaction of RSNO-Cl with subsurface poly(HEMA) block to get (#10) H(N)-*b*-S. (C) SEM characterizations (scale bar = 10 μm): surface and cross section (inset) of (i) (#1) unmodified PU and (ii) (#10) H(N)-*b*-S. (D) 3D AFM characterization of (i) unmodified PU catheter and (ii) (#10) H(N)-*b*-S. (E) Water contact angle change of (#10) H(N)-*b*-S over 1-month incubation in water. (F) HPLC detection of NO release precursor (NTMB-Cl) leaching to different solvents (N.D. refers to no detection of leaching). (G) NO release flux of (#10) H(N)-*b*-S coating at 37 °C over 15 days.

2B(iv)), the disappearance of the poly(HEMA) brush C−O−H groups signal (at 1020 cm^{-1}) corroborates the successful reaction between C−O−H groups of (#7) and the chloride group of the NO-donor (NTMB-Cl). For (#10) (Figure 2B(iv)), the ester carbonyl signal (1742 cm^{-1}) was further increased, corroborating the successful reaction of the chloride group of NTMB-Cl with hydroxyl groups of poly(HEMA).

With scanning electron microscopy (SEM) (Figure 2C), the cross-section of the (#1) uncoated catheter was almost featureless but that of (#10) H(N)-*b*-S coated catheter showed a stratified coating with a total thickness of about 10 μm; the subsurface bottom layer was estimated to be 3−5 μm thick from examining the first poly(HEMA) block that is quenched after one-step RAFT (Figure S4). 3D atomic force microscopy

https://dx.doi.org/10.1021/acscentsci.0c00755
ACS Cent. Sci. 2020, 6, 2031−2045

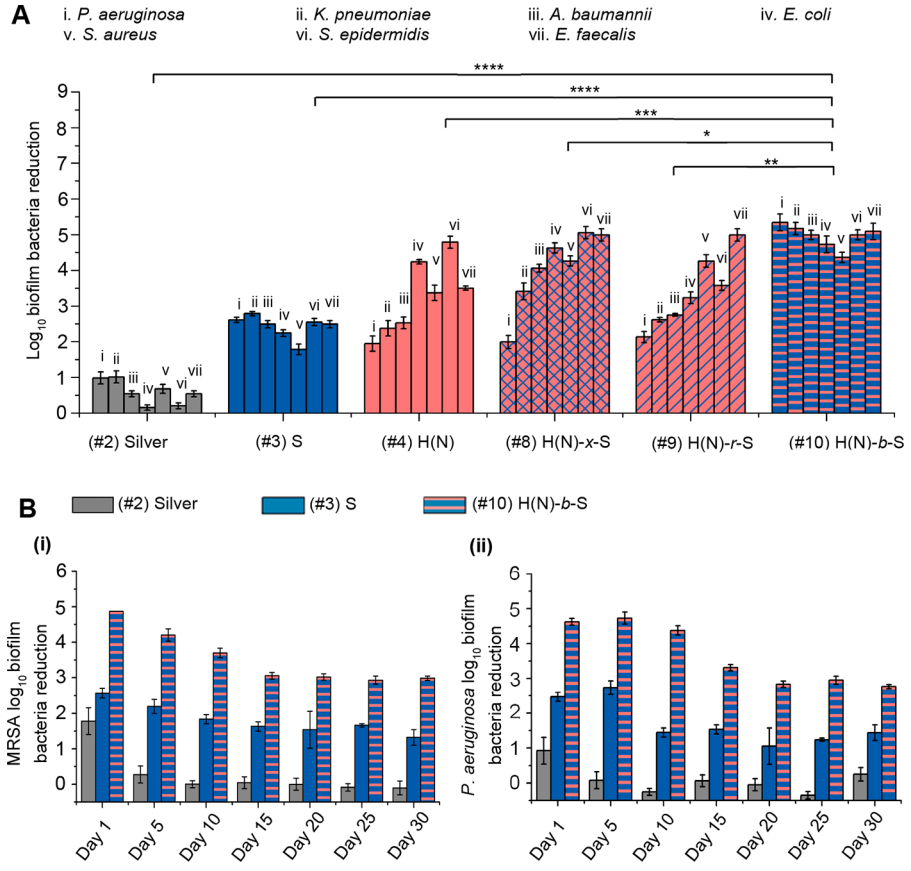

Figure 3. (A) 24 h-anti-biofilm efficacy of coatings measured by static media model against broad-spectrum Gram-negative and Gram-positive bacteria. The general log reduction of #10 is compared with other catheter coating controls by Student's *t* test, ****$P < 0.0001$, ***$P < 0.001$, **$P < 0.01$, *$P < 0.05$. (B) Long-term (30 days) intraluminal antibiofilm effect against (i) MRSA and (ii) *P. aeruginosa* bacteria.

(AFM) image of (#10) H(N)-*b*-S coated surface indicated that the block copolymer coating was very dense and thick with full coverage of the PU substrate (Figure 2D). The (#10) H(N)-*b*-S coating was very smooth with measured root-mean-square (RMS) roughness of 15.4 ± 3.4 nm and superhydrophilic with superlow water contact angle (8.0 ± 0.4°, Figure 2E) compared to the unmodified PU control (83.7 ± 0.3°, Figure 2E). The (#10) H(N)-*b*-S brush coating was also chemically stable as proven by the inconsequential increase of contact angle (<10.0°) when incubated in water (Figure 2E) and various media (PBS, serum, and bacterial inoculum, Figure S5A–D) for 1 month. To assess the leachability of the grafted NO-donor, (#10) H(N)-*b*-S coated catheter was extracted with PBS solution, polar (methanol) and nonpolar (hexane) solvents for 24 h and 1 week (Figure 2F); no leaching of the NO-donor was detected in the 341 nm absorbance measurements. These nonleaching results prove the long-term stability of the grafted polymer coating (#10). Further, the flux of released NO from (#10) catheter at 37 °C (Figure 2G) can be maintained over 15 days (375 h) at higher than the endogenous NO flux level from epithelial cells.[24] The density of NO-release precursors grafted on catheter is estimated to be 2.02×10^{-6} mol per cm^2 (Supporting Information Figure S4C).

The FTIR and physical characterizations of other coatings (#3 to #9) corroborated their successful syntheses (Figure S6A to Figure S12A). The random (#8) and cross-linked (#9) RSNO-containing coatings have a higher roughness, shown under SEM and AFM, with surface RMS roughness >100 nm (Figure S11B(i–ii) and S12B(i–ii)) and are much more hydrophobic, with contact angles >70° (Figures S11B(iii) and S12B(iii)). The RSNO donor is also not leachable from either the random (#8) (Figure S11C) or the cross-linked (#9) coatings (Figure S12C), and the RSNO donor grafting density for cross-linked (#8) and random (#9) coatings are estimated to be 2.75×10^{-6} mol per cm^2 (Figure S11D) and 2.03×10^{-6} mol per cm^2 (Figure S12D) respectively.

2.3. Excellent Antibacterial and Antibiofilm Efficacy of (#10) Brush Coating. The acute (2 h) antibacterial efficacies of all the catheters (#2 to #10) were tested. Among them, only NO-emitting catheters (#4, #8, #9, and #10) achieve substantial ($\geq 2.0 \log_{10}$, ≥99.0%) antibacterial efficacy against all pathogens tested, specifically Gram-positive (Figure S13) methicillin-resistant *Staphylococcus aureus* (MRSA BAA40), methicillin-resistant *Staphylococcus epidermis* (MRSE ATCC 35984), and vancomycin-resistant *Enterococcus faecalis* (VRE V583), as well as Gram-negative (Figure S13) *Pseudomonas aeruginosa* (PAO1), *Klebsiella pneumoniae* (ATCC 13883), *Acinetobacter baumannii* (ATCC 19606), and *Escherichia coli* (UTI189). The antibacterial efficacies of these NO-emitting catheters (#4, #8 to #10) were comparable to the silver coating control (#2). The purely hydrophilic coatings (#3, #5 to #7) had no antibacterial effect. Hence, NO-emission function is important for achieving an antibacterial effect that would prevent bacterial colonization.

The short-term (24 h) antibiofilm efficacy of the coatings (#2) to (#10) were also evaluated, and only (#10) the diblock copolymer brush with NO-release functionality and a hydro-

https://dx.doi.org/10.1021/acscentsci.0c00755
ACS Cent. Sci. 2020, 6, 2031–2045

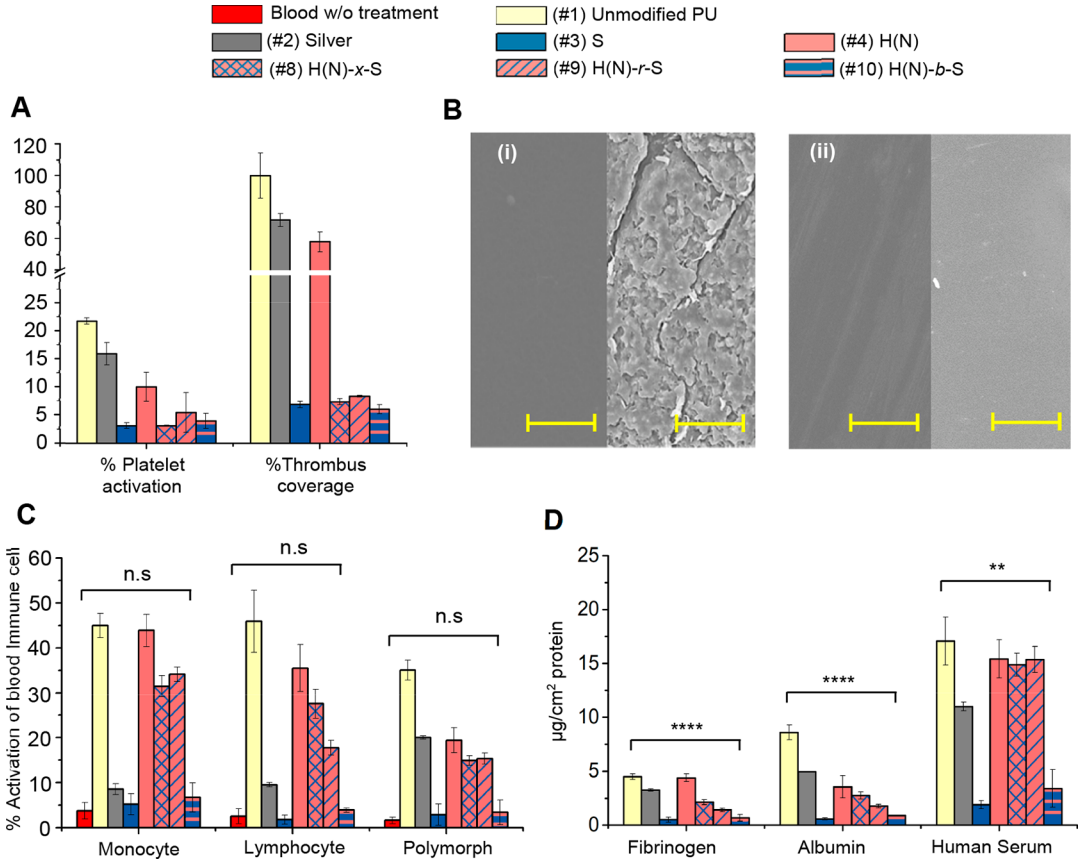

Figure 4. Biocompatibility and hemocompatibility of coatings: (A) Antithrombogenic effect of coatings measured by platelet activation and amount thrombus formation. (B) SEM images of thrombus formed on catheters (Left: before incubation with rabbit whole blood. Right: after 2 h incubation with rabbit whole blood) (i) (#1) unmodified catheter, (ii) (#10) H(N)-*b*-S (scale bar = 10 μm). (C) Activation of blood immune cells. Student's *t* test of #10 against blood w/o treatment, n.s. $P > 0.05$. (D) Blood protein fouling on catheters after 24 h incubation with protein or serum. Student's *t* test of #10 against unmodified catheter, ****$P < 0.0001$, **$P < 0.01$.

philic surface layer could achieve >4.0log$_{10}$ inhibition against both Gram-positive and Gram-negative (Figure 3A(i)) bacteria tested. Comparing the purely hydrophilic coatings (#3, #5−7), only (#3) and (#7) brushes with surface poly(SBMA) layer seem to perform slightly better than (#5) and (#6), by 0.5−1.5log$_{10}$ orders of magnitude, against both the Gram-positive and Gram-negative bacteria (Figure S14A). Comparing the NO-releasing coatings (#4, #8-#10), they were all effective against all the Gram-positive species tested (Figure 3A(i)). However, against the entire panel of Gram-negative bacteria tested (*P. aeruginosa, K. pneumoniae, A. baumannii*, and *E. coli*) (Figure 3A(i)), (#10) is the only NO-emitting coating that achieved 4.7−5.3log$_{10}$ inhibition. The (#9) NO-emitting random copolymer has generally poor (2.1 to 2.8log$_{10}$) inhibition against the Gram-negative bacteria except *E. coli* (with 3.2log$_{10}$ reduction). The (#8) NO-emitting hydrogel has poor to moderate (2.0 and 3.4log$_{10}$) reductions of *P. aeruginosa* and *K. pneumoniae*, which were about 2.0log$_{10}$ less than (#10); it has good (4.1 and 4.6log$_{10}$) reduction against the specific bacteria of *A. baumannii* and *E. coli*.

The *in vitro* efficacy of #8 to #10 against four multidrug resistant strains was tested before the *in vivo* studies. The multidrug resistant Gram-negative clinical isolates obtained from Tan Tock Seng Hospital (TTSH, Singapore) were the following: pan-resistant *Pseudomonas aeruginosa* (PAER), carbapenem-resistant *Klebsiella pneumoniae* (KPNR), multi-drug resistant (MDR) *Acinetobacter baumannii* (AB-1), and MDR *Escherichia coli* (ECOR-1). The NO-release block copolymer coating (#10) shows 4.7−5.0log$_{10}$ inhibition of biofilm formation against various MDR Gram-negative bacteria, which is 93−98% more potent than the cross-linked NO-release coating (#8), and 97−99.7% more potent than the random NO-release coating (#9) (Supporting Figure S14B).

The MRSA and *P. aeruginosa* bacteria adhesion on various catheters after 24 h incubation were also observed with fluorescence microscopy (Figure S14C). On the (#10) coated catheter surface, neither MRSA or *P. aeruginosa* was found, while on (#1) unmodified, (#4) purely NO-emitting and (#7) purely hydrophilic coatings both MRSA and *P. aeruginosa* bacteria were found to various extents. Hence, of the various NO-emitting formulations, only (#10) H(N)-*b*-S with an antifouling surface layer and a hidden subsurface NO-donor layer achieves excellent (4.4−5.3log$_{10}$) antibiofilm effect against both Gram-positive and Gram-negative bacteria. Coating (#10) H(N)-*b*-S, is the most effective of the tested coatings in terms of antibacterial and antibiofilm effect for the broad spectrum of bacteria tested.

We also evaluated the *in vitro* long-term (30 days) antibiofilm properties of 30 cm long (#10) coated catheter and compared it with a few controls, i.e., (#1) uncoated, (#2) silver-coated, and (#3) poly(SBMA)-coated catheters, using a homemade intraluminal circulatory setup (Figure S14D) with a biofilm-promoting medium. For both MRSA and *P. aeruginosa* (Figure 3B(i) and (ii)), the (#2) silver-coated

https://dx.doi.org/10.1021/acscentsci.0c00755
ACS Cent. Sci. 2020, 6, 2031−2045

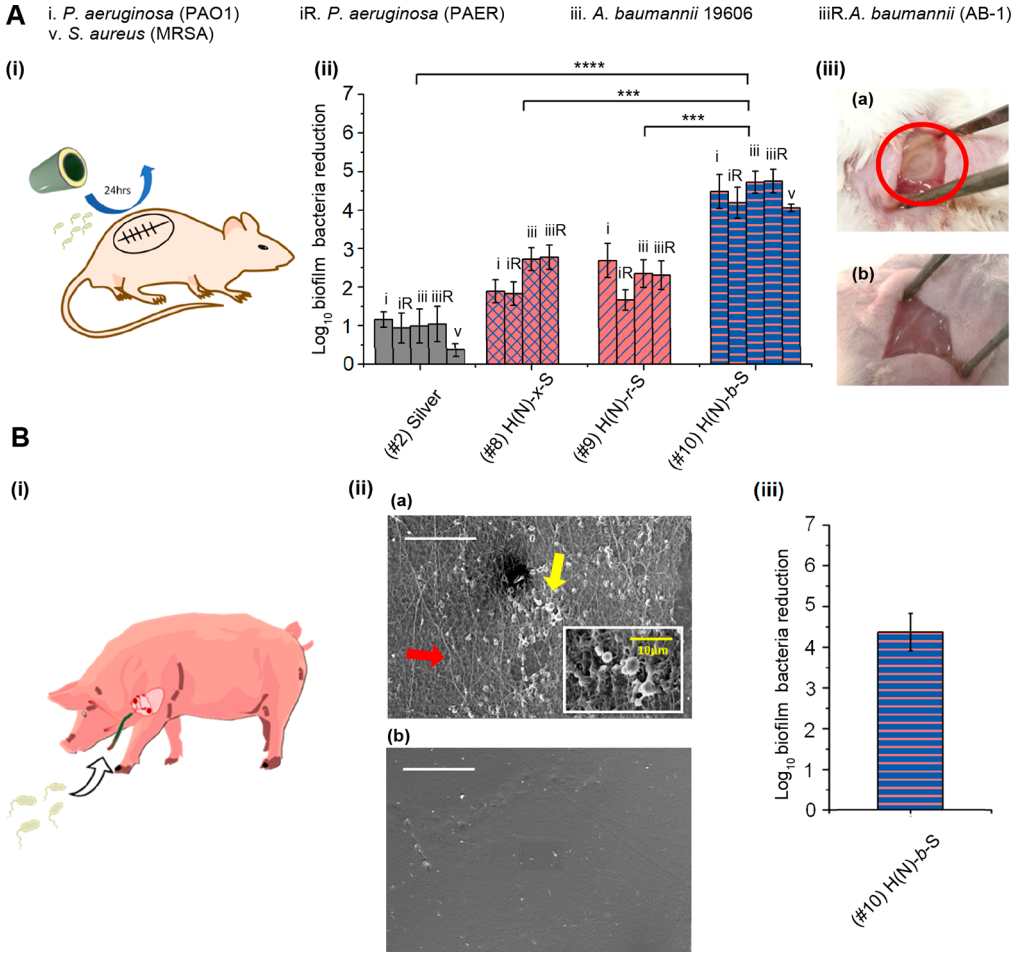

Figure 5. *In vivo* antibacterial efficacy of coated catheters: (A) Murine subcutaneous 24 h implantation infection model (i) illustration of subcutaneous implantation and infection, (ii) antibiofilm efficacy of catheters (#8, #9, and #10) against antibiotic-sensitive and multidrug resistant (MDR) bacteria, (iii) appearance of MDR PAER infected subcutaneous pockets after 24 h implantation. (a) pus (red circle) found in the subcutaneous pocket implanted with (#1) unmodified catheter (b) minimal pus found in the subcutaneous pocket implanted with (#10) H(N)-*b*-S catheter. The general log reduction of #10 is compared with other catheter coating controls by Student's *t* test, (#2) silver catheter, $^{****}P < 0.0001$, (#8) catheter, $^{***}P < 0.001$, (#9) catheter, $^{**}P < 0.01$. (B) Porcine central venous catheter model with MRSA: (i) illustration of catheter implantation in porcine jugular vein and infection Pig III, (ii) biofilm (yellow arrow, and subfigure) and thrombus formation (red arrow) on catheters observed under SEM (scale bar = 50 μm) with (a) (#1) unmodified PU catheter (b) (#10) H(N)-*b*-S catheter. (iii) antibiofilm efficacy of catheter (#10) H(N)-*b*-S.

catheter showed limited initial (day 1) antibiofilm efficacy (~90% inhibition) but developed biofilm from day 5 onward. The purely hydrophilic coating (#3) showed a moderate 30-day antibiofilm effect with 1.6 and 1.5log$_{10}$ inhibitions for MRSA and *P. aeruginosa* respectively. The (#10) H(N)-*b*-S coating retained about 99.9% inhibition against both MRSA (3.1log$_{10}$ inhibition) and *P. aeruginosa* (3.0log$_{10}$ inhibition) after 30 days. This study proved the excellent *in vitro* long-term (30 days) efficacy of (#10) H(N)-*b*-S and is the first report of a catheter coating with such high (around 3.0log$_{10}$) long-term (30 days) antibiofilm effect against both Gram-positive and Gram-negative bacteria.

2.4. Excellent Biocompatibility. All control and coated catheters (#1 to #10) showed no toxicities toward all tested mammalian cell lines: 3T3 fibroblasts, human embryonic kidney (HEK 293) cells, human liver hepatoma (HepG2) cells, and human dermal fibroblasts (Figure S15A). Upon incubation with rabbit whole blood for 2 h, the (#1) unmodified catheter (Figure 4A) produced 22.5% activation of platelets and was densely covered with thrombi (Figure 4B(i)). This level was set as the 100% thrombus formation control mark for comparison with other coatings. The (#2) silver-coated catheter showed 15.1% platelet activation and 73.2% thrombus formation. The purely NO-emitting coating (#4) (Figure 4A) showed moderate platelet activation (~10%) and significant (58.6%) thrombus formation. The purely hydrophilic and the hydrophilic NO-coated catheters ((#3, #5 to #10, Figure 4A and Figure S15B) showed low platelet activation (<10% activation), and low thrombus formation (<10%). SEM of (#10) H(N)-*b*-S coated catheter exposed to rabbit blood revealed a clean surface with no thrombus formation (Figure 4B(ii)).

The (#1) unmodified PU catheter (Figure 4C) triggered significant activation of immune cells (i.e., monocytes (45%), lymphocytes (48%), and polymorphs (34%)). The (#2) silver-coated catheter (Figure 4C) also triggered a substantial degree of activation of monocytes (8.2%), lymphocytes (9.5%) and polymorphs (20.0%). The purely hydrophilic coatings (#3, #5 to #7) triggered low levels (2–6%) of immune cell activation which were only slightly higher than the endogenous level (1–

https://dx.doi.org/10.1021/acscentsci.0c00755
ACS Cent. Sci. 2020, 6, 2031−2045

4%, red bars, Figure S15C) of blood immune cell activation in the absence of trigger (negative control, i.e., blood without treatment). Interesting, the NO-donor modified random copolymer (#8) and cross-linked hydrogel (#9) show significant levels (20−30%) of activation of immune cells (Figure 4C) compared with their parent non-NO emissive purely hydrophilic coatings (#5, #6). On the other hand, the NO-emitting diblock copolymer brush coating (#10) (Figure 4C) showed low activation levels for lymphocytes (6.4%), monocytes (3.9%), and polymorphs (3.7%), which was comparable to the endogenous levels. The hydrophobic NO-donor which is hidden in the subsurface poly(HEMA) avoids contact with immune cells and reduces their activation compared with alternative coating structures.

We evaluated the protein fouling resistances of the coatings by incubating the catheters with 1% fibrinogen, 10% albumin, and 50% human serum, which contains a complex mixture of blood proteins (Figure 4D and Figure S15D). The (#1) unmodified, (#2) silver-coated, and (#4) H(N)-coated catheters all experienced high protein fouling, corresponding to their high contact angles (83.7°, 80.8°, and 87.8° respectively) (Figure 2E and Figure S7B), which mirror the trend of immune cell activation. All the purely hydrophilic coatings (#3, #5 to #7) exhibited reduced fouling with <0.5 $\mu g/cm^2$ for fibrinogen, <1 $\mu g/cm^2$ for albumin, and <4 $\mu g/cm^2$ for human serum. For catheters functionalized with NO-donor, only (#10) (and not #8 and #9) exhibits low protein fouling. As with the immune cell exposure, (#10) H(N)-*b*-S coated catheter, which has a hydrophilic antifouling poly(SBMA) surface layer, could resist protein fouling to achieve comparable protein resistance to non-NO-release purely hydrophilic (#7) H-*b*-S coating (Figure 4D).

2.5. *In Vivo* Murine and Porcine Models of Catheter-Associated Infections. *In vivo* performance of the coatings was assessed in a murine subcutaneous catheter implantation infection model[28] and a porcine central venous catheter (CVC) infection model[29] (Figure 5). In the murine subcutaneous infection model, the NO-release catheters (#8) H(N)-*x*-S, (#9) H(N)-*r*-S, (#10) H(N)-*b*-S, and the (#1) unmodified catheter control were first infected with high concentrations of *P. aeruginosa* or *A. baumannii* (10^6CFU/mL) and then implanted into subcutaneous pockets created on the backs of mice (Figure 5A(i)). Both antibiotic-sensitive and antibiotic-resistant *P. aeruginosa* (PAO1 and PAER) or *A. baumannii* (ATCC 19606 and AB-1) were investigated. 24 h after implantation, the catheters were removed. The (#10) H(N)-*b*-S coated catheter achieved excellent (>4.0$\log_{10}$) antibiofilm effect against both *P. aeruginosa* and *A. baumannii* compared with less than 1.0$\log_{10}$ inhibition with silver (#2 (Figure 5A(ii)). The (#10) H(N)-*b*-S also shows 1.8−2.6$\log_{10}$ better potency than the cross-linked hydrogel and random copolymer NO-release coatings ((#8) and (#9)) against *P. aeruginosa* and *A. baumannii*, including multidrug resistant clinical isolates (Figure 5A(ii)). The (#10) H(N)-*b*-S coated catheter also achieved excellent (4.1$\log_{10}$) antibiofilm effect against Gram-positive MRSA compared with less than 1.0$\log_{10}$ inhibition with silver (#2) (Figure 5A(ii)). The importance of block copolymer arrangement for *in vivo* application is corroborated by the mice subcutaneous infection model. The pocket implanted with (#1) unmodified PU control catheter showed a yellowish mass of pus which was indicative of infection and inflammation (Figure 5A(iii)a, red circle), while the pocket implanted with (#10) H(N)-*b*-S catheter was almost clean and without any visible signs of inflammation (Figure 5A(iii)b).

We also tested (#10) H(N)-*b*-S catheter in a porcine central venous catheterization (CVC) model[29] in three pigs (Figure 5B). The *in vivo* biocompatibility of coated catheter (#10) versus uncoated catheter (#1), both of which were without infection, was first evaluated. Pig I and Pig II which were both uninfected were implanted with either (#1) unmodified catheter or (#10) H(N)-*b*-S coated catheter, respectively. There was no significant difference in the mean arterial blood pressure (MAP) of Pig I versus Pig II on the first day, third day, fifth day and seventh day time-points after catheter implantation (Supporting Figure S16Ai) (At these longer time points after surgery, the pigs were awoken from the anesthesia). The heart rates (HR) of both (uninfected) pigs implanted with (#1) unmodified catheter and (#10) H(N)-*b*-S coated catheter were also in the normal range, corroborating no long-term systemic toxicity of NO-releasing catheter (#10 H(N)-*b*-S) on the pigs (Figure S16Aii). Pig III was implanted with two catheters that were both dosed with MRSA bacteria (the left jugular vein with (#1) unmodified catheter and the right jugular vein with #10 coated catheter). The long-term blood pressure (MAP) and heart rate (HR) of the infected Pig III implanted with (#10) coated and (#1) unmodified catheters were also normal (Figure S16Ai and ii) (This pig was euthanized on day 5 to obtain the antibacterial efficacy results (Figure 5B)). Considering all the 3 pigs' results, our #10 coated catheters shows no long-term systemic toxicity (for day 1 to day 7).

However, when the pigs were under recovery from anesthesia (i.e., during the first 5 h after implantation, Figure S16B), a transient drop in MAP was observed. The MAPs of both uninfected Pig I and Pig II which were implanted with (#1) unmodified catheter and (#10) H(N)-*b*-S catheter respectively, generally dropped right after surgery until the second hour. Though the measured MAP of (uninfected) Pig II implanted with (#10) H(N)-*b*-S catheter at the second hour time point (81.3 ± 9.2 mmHg) was slightly below the normal lower limit of MAP (84 mmHg), its blood pressure recovered after that. However, the MAP of Pig III which was implanted with (infected) (#10) coated catheter during the anesthesia period (Figure S16B) was quite steady and above the lower normal limit. Though we cannot rule out the possibility of transient systemic toxicity of NO combined with anesthesia, proper dosing of NO and anesthesia or delayed NO release shall ensure the transient safety of NO-donor coated catheters during surgery.

To further evaluate the *in vivo* antibiofilm efficacy of catheters, 10 cm lengths each of (#1) unmodified PU catheter and (#10) H(N)-*b*-S coated catheter were prepared and implanted in the left and right jugular veins, respectively, of the same pig (Pig III) for unbiased comparison. MRSA (BAA-40) was then introduced to each catheter by dipping the external catheter terminal into bacteria inoculum in PBS (2×10^7CFU/mL) (Figure 5B(i)). The catheter was then plugged, and the wound and catheter were covered with sterile dressings. After 5 days of implantation, the pig was sacrificed, and the implanted catheters were removed and evaluated with SEM (Figure 5B(ii)). The inner surface of (#1) unmodified catheter (Figure 5B(ii)a) shows significant adhesion of MRSA (yellow arrow, and subfigure) and thrombi formation with activation of fibrinogen (red arrow) while (#10) H(N)-*b*-S coated catheter (Figure 5B(ii)b) shows clean surface without any trace of

https://dx.doi.org/10.1021/acscentsci.0c00755
ACS Cent. Sci. 2020, 6, 2031−2045

biofilm or thrombus development and fibrinogen adhesion. The number of bacteria colonizing the surfaces of the catheters were quantified (Figure 5B(iii)); the (#10) H(N)-*b*-S coated catheter showed 4.4log$_{10}$ reduction of biofilm bacteria compared with (#1) unmodified PU catheter. The (#10) H(N)-*b*-S coated catheter showed excellent *in vivo* antibiofilm, antithrombus formation efficacy and biocompatibility.

3. DISCUSSION

The bacteria that infect medical devices in clinical settings are broad spectrum, and our seven tested bacteria are highly relevant.[30] We have shown that (#10) H(N)-*b*-S diblock brush covalently grafted from PU catheter surface achieves excellent short-term and long-term *in vitro* broad-spectrum antibiofilm effect against both Gram-positive and Gram-negative bacteria. For the 24 h *in vitro* test, it achieves 99.99% to 99.999% (4.0−5.0log$_{10}$) reduction of all seven Gram-positive and Gram-negative bacteria tested, while all other coatings, including (#2) silver and (#3) zwitterionic polymer brushes which are well-explored by others, could only achieve less than 99.9% (3.0log$_{10}$) reduction against the same bacterial range. In a murine subcutaneous infection model, (#10) coating achieves 99.9955% (4.1log$_{10}$) and 99.9973% (4.8log$_{10}$) reduction of MRSA and *P. aeruginosa* biofilm respectively, while silver catheter achieves respectively 68% and 84% (0.5 and 0.8log$_{10}$) reduction of these 2 bacteria. Further, in a porcine CVC infection model, (#10) achieves excellent *in vivo* medium-term antibiofilm effect of greater than 99.99% (4.4log$_{10}$) inhibition of MRSA after 5-day implantation with good biocompatibility (Figure 3, Figure 4, and Figure 5).

Against the Gram-positive bacteria, the NO-emitting coatings (#4, #8, #9, and #10) show >3.0log$_{10}$ inhibition. However, against the four Gram-negative bacteria, coating (#10) stands out as distinctly superior to the other coatings, with >4.7log$_{10}$ inhibition against all tested pathogens; some of the other coatings approach this performance against individual pathogens, but against the group none is nearly as effective as (#10). The non-NO-emitting coatings ((#3) S, (#5) H-*x*-S, (#6) H-*r*-S, and (#7) H-*b*-S) have inferior antibiofilm effect against all bacteria with 1.8−2.9log$_{10}$ inhibition compared with (#10) (4.4−5.3log$_{10}$) (Figure S14A). Of the 3 differently structured NO-releasing coatings (#8, #9, #10), only the precision diblock copolymer (#10) has good broad spectrum antibiofilm effect with excellent blood compatibility (Figures 3 and 4). Both cross-linked and random copolymer brush coatings ((#8) and (#9), Figure S11 and S12), which do not sequester the NO-release agent below the surface, show poor antibiofilm effect against some Gram-negative bacteria, higher activation of immune cells and more fouling with blood protein.

The covalent attachment of RSNO to the grafted brush coating prevents leaching of RSNO (Figure 2E) and results in sustained NO flux over 15 days (Figure 2F) that is about 1 order of magnitude higher than reported values with blending.[24] Blending of RSNO with a polymer coating without covalent bonding would result in leaching with ensuing toxicity and shorter sustained release.[24] Both cross-linked and random copolymer brush coatings ((#8) and (#9), Figures S11 and S12), which do not sequester the NO-release agent below the surface, are more hydrophobic than their non-RSNO-functionalized counterparts ((#5) and (#6), Figures S8 and S9). The sequestration of hydrophobic RSNO in the subsurface block of (#10) H(N)-*b*-S does not degrade the hydrophilicity of the outer hydrophilic poly(SBMA) block as shown by its still small contact angle (8.0 ± 0.4°, Figure 2D). The combination of surface hydrophilicity and NO emission is necessary to effectively inhibit biofilm by a broad spectrum of pathogens.

Further, the (#8) cross-linked and (#9) random copolymer coatings made by free-radical copolymerization have much higher roughness than (#10) block copolymer brush coatings made by controlled RAFT copolymerization. The RSNO decomposes to thiyl radicals (RS•) after the release of the NO molecule which may reduce the biocompatibility of the coating.[31,32] The disulfide bonds formed from two adjacent RSNO molecules that had released their NO molecules are potentially still bioactive toward thiol-containing proteins.[33] The coatings (#8) and (#9) will expose these radicals or disulfide bonds which would activate immune cells (Figure 4C) or cause protein fouling (Figure 4D) as opposed to block copolymer coating (#10) that has a nonimmune active nature. The block copolymer coating with a hydrophilic layer (#10) sequesters the thiyl radicals (RS•) and disulfide bond to prevent activation of any immune cells or protein fouling (Figure 4C,D). The higher hydrophilicity, lower surface roughness and reduced surface bioactivity of (#10) prevent blood protein fouling and thrombus formation, reduces immune activation[34] and result in less attachment of bacteria and proteins. The sequestration of RSNO in the subsurface block in (#10) is important to the multifunctionality of this coating.

Our precision (#10) diblock copolymer is made by the ozone-surface-RAFT technique. The ozone treatment creates a high areal density of peroxide initiator (169 peroxide initiators/nm^2, Supplementary Equation S1[35]) on both the inner and outer surfaces of even slender catheters. Further, the surface-initiated polymer brush is chemically bonded to the catheter material, which is a more robust attachment than previously reported initiator impregnation method which results in unstable brush coating as shown by reversion of contact angle after 14 days.[14] Our technique enables the creation of a uniform, dense, and precisely structured block copolymer brush achieving outstanding functionality. It is readily applicable to the surface modification of catheters at scale and, more generally, is applicable to the formation of controlled multifunctional coatings on complex and relatively inaccessible surfaces of a wide range of medical devices.

4. CONCLUSION

We have demonstrated a precision-structured diblock brush coating (#10) H(N)-*b*-S that achieves excellent short-term and long-term antibiofilm effects against Gram-negative and Gram-positive bacteria with excellent blood compatibility. It outperforms other previous coatings that are purely hydrophilic or have exposed NO-donor. The precise placement of the surface antifouling block and the subsurface NO-emitting block is critical for achieving excellent antibiofilm effect with excellent thrombus formation resistance and biocompatibility. The (#10) H(N)-*b*-S coating achieves excellent 4.4−5.3log$_{10}$ short-term (24 h) inhibition of biofilm formation in seven clinically relevant Gram-positive and Gram-negative bacteria and outperforms (#2) silver and (#7) purely hydrophilic by around 4.0log$_{10}$ and 2.0log$_{10}$ respectively. The (#10) H(N)-*b*-S is the first report of a catheter coating that can cover clinically useful (30 cm) lengths with excellent long-term reduction (3.0log$_{10}$ at 30th day) of MRSA and *P. aeruginosa* biofilm in an intraluminal *in vitro* model. In a murine subcutaneous catheter

https://dx.doi.org/10.1021/acscentsci.0c00755
ACS Cent. Sci. 2020, 6, 2031−2045

infection model, this coating achieves greater than 4.0$\log_{10}$ inhibition of Gram-positive MRSA and Gram-negative *P. aeruginosa*, and *A. baumannii* respectively. Further, we show for the first time a catheter coating with excellent antibiofilm efficacy in an *in vivo* central venous infection model.

The ozone-surface-RAFT coating method developed in this work shows great potential to achieve high-performance, anti-infective coatings on other medical devices, which, like catheters, require coatings that are multifunctional, non-leaching, and long-term biofilm-resistant. Like catheters, many such devices are difficult to uniformly coat, and our method should be applicable to them. The H(N)-*b*-S coating may have a transformative impact in greatly reducing infections associated with catheter use in healthcare settings and in a wide range of biomedical devices, including those with challenging shapes and multifaceted requirements.

5. EXPERIMENTAL SECTION

5.1. Materials. Polyurethane catheter (Micro-Renathane Tubing) with inner/outer diameter: 2.0 mm/3.5 mm was purchased from Braintree Scientific. 2-Hydroxyethyl methacrylate (>99%) (HEMA), [2-(methacryloyloxy) ethyl] dimethyl-(3-sulfopropyl) ammonium hydroxide (sulfobetaine methacrylate, SBMA), triethylene glycol dimethacrylate (TEGDMA), ammonium iron(II) sulfate (Mohr's salt), 4-cyano-4-(phenylcarbonothioylthio) pentanoic acid (CPCPA, chain transfer agent), 4,4′-azobis(4-cyanovaleric acid) (ACVA, thermal initiator), butylamine, oxalyl chloride, *tert*-butyl nitrite, 3-mercapto-3-methylbutan-1-ol, 3-(4,5-dimethylthiazol-2-yl)-2,5-diphenyltetrazolium bromide (MTT), fibrinogen, albumin, and human serum were purchased from Sigma-Aldrich and used without further purification. Ozone was generated with an Arzocon RMU16-K3 using air as O_2 source. Polyurethane catheter (#1) control was used as received. Silver-coated catheter (#2) was purchased from a commercial supplier (confidential).

Bacteria: Methicillin-resistant *Staphylococcus aureus* (MRSA) BAA-38 and BAA-40, vancomycin-resistant *Enterococci* (VRE) V583, methicillin-resistant *Staphylococcus epidermidis* (MRSE) 35984, *Pseudomonas aeruginosa* PAO1, *Acinetobacter baumannii* 19606 and *Klebsiella pneumoniae* 13883 were obtained from ATCC. *Escherichia coli* UTI89 was donated by another research group. Clinically relevant multi-drug resistant (MDR) Gram-negative bacteria *E. coli* (ECOR-1), *A. baumannii* (AB-1), *P. aeruginosa* (PAER), and *K. pneumoniae* (KPNR-1) were obtained from Tan Tock Seng Hospital (TTSH), Singapore.

5.2. Experiments. *5.2.1. Surface Analysis.* The surface functional groups of modified catheters were characterized using a Fourier-transform infrared spectrometer (FTIR) with ATR accessory at an incident angle of 90° (Nicolet 5700, Thermo Fisher Scientific, U.S.A). Water contact angles were measured with a drop shape analyzer, DSA-25, Kruss Scientific, Germany. Surface morphologies of the catheters were studied with scanning electron microscopy (JEOL JSM-6701F, Japan) and atomic force microscopy (Bruker Dimension Icon).

5.2.2. Ozone Treatment of Polyurethane Catheter (5 mm). Unless otherwise specific, all the catheters used were 5 mm in lengths and have inner and outer diameters of 2.0 mm and 3.5 mm, respectively. The surface coated catheters were all subjected to the ozone pretreatment as described here. Polyurethane (PU) catheter was sectioned into 5 mm long pieces, which were cleaned with methanol followed by deionized water. Ambient air was used as input to the ozone generator and the output ozone was purified by passing it through a 15 cm sodium hydroxide column. The cleaned PU catheter pieces were put in a conical flask with ozone flowing into the flask at 0.6 L/min for 30 min to introduce peroxide groups. The ozone treated PU catheters were put under vacuum conditions (<10 Pa) at room temperature for 1 h to remove oxygen/ozone diffused into the PU.

5.2.3. Titration of Peroxide Group on Ozone-Treated Polyurethane Catheter. The concentration of surface peroxide groups was titrated against sodium thiosulfate following Keiji's protocol.[35] 25 mL of IPA was added to the ozone treated catheter, followed by 1 mL of saturated KI solution with 1 mL of acetic acid. The mixture was heated and kept at boiling point for 5 min with constant stirring by a magnetic bar and titrated with 0.01 mM $Na_2S_2O_3$ until the yellow color completely change to white. The calculation procedure of surface peroxide group density is summarized in eq S1.

5.2.4. Synthesis of Homo Poly(SBMA) Coating ((#3) S) on PU Catheter (Figure S1A). 10 wt % of SBMA solution in 10 mL of water and isopropanol (IPA) mixture (1:1 v/v)) was prepared. The monomer solution was purged in a Schlenk tube using argon for 30 min. The ozone-treated 5 mm long catheters were then put into the monomer solution, and the solution was further purged for 5 min. Then, 8 mg of ammonium iron(ii) sulfate ($(NH_4)_2Fe(SO_4)_2{\cdot}6H_2O$, Mohr's salt) was added to initiate the surface-initiated free radical polymerization. The polymerization reaction was carried for 24 h at room temperature. The coated PU catheter was washed and sonicated in DI water to remove unreacted monomer and homopolymer formed.

5.2.5. Synthesis of RSNO-Modified Homo Poly(HEMA) ((#4) H(N)) on Catheter Pieces (Figure S1B). 5.2.5.1. Synthesis of Poly(HEMA)-Coated Catheter. 5 wt % of HEMA solution in 10 mL of water and isopropanol (IPA) mixture (1:1 v/v)) was prepared. The monomer solution was purged in a Schlenk tube using argon for 30 min. The ozone-treated 5 mm long catheters were then put into the monomer solution, and the solution was further purged for 5 min. Then, 8 mg of ammonium iron(ii) sulfate ($(NH_4)_2Fe(SO_4)_2{\cdot}6H_2O$, Mohr's salt) was added to initiate the surface-initiated free radical polymerization. The polymerization reaction was carried out for 24 h at room temperature. The polyHEMA-coated PU catheter was washed and sonicated in DI water to remove unreacted monomer and homopolymer formed.

5.2.5.2. Grafting of RSNO to Coating. The synthesis of NO release precursor followed the scheme above (Scheme S1). 1.2 g of 3-mercapto-3-methylbutan-1-ol was dissolved in 10 mL of cold ether, and 1.03 g of *tert*-butyl nitrite was added dropwise; the mixture was reacted for 30 min at 0 °C for full conversion of the nitroso group. The reaction solution was then purified with partial vacuum to remove byproduct and ether. The product, *S*-nitroso-3-mercapto-3-methylbutan-1-ol, was then quickly dissolved in 10 mL of hexane, with addition of 1.39 mL of triethylamine; this mixture was maintained at 0 °C. 0.84 mL of oxalyl chloride was dissolved in 5 mL of hexane and added dropwise to the chilled *S*-nitroso-3-mercapto-3-methylbutan-1-ol solution; the mixture was reacted at 0 °C for 2 h to obtain *S*-nitroso-3-mercapto-3-methylbutan-1-chloride.

The poly(HEMA) coated were then added into prepared *S*-nitroso-3-mercapto-3-methylbutan-1-chloride (NTMB-Cl) solution (10w/w% in hexane) and reacted with it for 12 h under ice-bath. The modified catheters were washed in methanol and

https://dx.doi.org/10.1021/acscentsci.0c00755
ACS Cent. Sci. 2020, 6, 2031−2045

water for 4 h at 0 °C to remove unreacted NTMB-Cl. The final coating (#4) H(N) was produced.

5.2.6. Synthesis of Cross-Linked Hydrogel Coating ((#5) H-x-S) on Catheter (Figure S2). For cross-linked hydrogel coating, solution containing monomer and cross-linker (5 wt % SBMA, and 5 wt % HEMA, and 1 wt % TEGDMA in 10 mL water and isopropanol (IPA) mixture (1:1 v/v)) was prepared. The solution was purged with argon in a Schlenk tube for 30 min. The ozone-treated 5 mm long catheters were then put into the monomer/cross-linker solution, and the solution was further purged for 5 min. Then, 8 mg of ammonium iron(ii) sulfate ($(NH_4)_2Fe(SO_4)_2{\cdot}6H_2O$, Mohr's salt) was added to initiate the surface-initiated free radical polymerization. The polymerization reaction was carried out for 24 h at room temperature. The coated PU catheters were washed and sonicated in DI water to remove unreacted monomer and unattached homopolymer formed.

5.2.7. Synthesis of Random Copolymer Coating ((#6) H-r-S) on Catheter Pieces (Figure S3). For the random copolymer brush coating, the solution containing monomers (5 wt % SBMA monomer and 5 wt % HEMA monomer in 10 mL of water and isopropanol (IPA) mixture (1:1 v/v)) was prepared. The solution was purged with argon in a Schlenk tube for 30 min. The ozone-treated 5 mm long catheters were then put into the monomer solution, and the solution was further purged for 5 min. Then, 8 mg of ammonium iron(ii) sulfate ($(NH_4)_2Fe(SO_4)_2{\cdot}6H_2O$, Mohr's salt) was added to initiate the surface free radical polymerization. The polymerization reaction was carried out for 24 h at room temperature. The coated PU catheters were washed and sonicated in DI water to remove unreacted monomer and homopolymer formed.

5.2.8. Synthesis of Precisely Structured Diblock Copolymer Coating ((#7) H-b-S) on Catheter Pieces (Figure 1C).
Step 1: Ozone activation (see Section 5.2.2).

Step 2: Grafting of the first block of chain transfer agent terminated poly(hydroxyethyl methacrylate) layer (poly(HEMA)) onto catheter.

10 wt % HEMA solution in 10 mL of water and ethanol (4:1 v/v) mixture was prepared. 10 mg of thermal initiator 4,4′-azobis(4-cyanovaleric acid) (ACVA) and 40 mg of chain transfer agent 4-cyano-4-(phenylcarbonothioylthio) pentanoic acid (CPCPA) were then dissolved in the solution. Additional thermal initiators are still needed in the monomer solution even though peroxide groups have already been introduced onto the surface.[25] The additional thermal initiators act as scavengers for trace of impurities that might otherwise terminated the polymer initiation.[26,36] The solution was purged with argon in a Schlenk tube for 30 min. The ozone treated 5 mm long catheters were then put into the monomer solution, the solution was further purged for 5 min, and the tube was sealed. The surface Ozone-surface-RAFT polymerization was initiated by heating to 70 °C. The polymerization reaction was carried out for 24 h and then quenched in an ice-bath. The coated PU catheter was washed and sonicated in pure ethanol to remove unattached homo poly(HEMA) and residual monomer.

Step 3: RAFT polymerization of second block of poly(SBMA) *to form the deblock brush covalently grafted from catheter* ((#7) H-*b*-S).

10 wt % solution of SBMA in water and ethanol mixture (4:1 v/v) was prepared. 10 mg of thermal initiator ACVA was dissolved in this solution. The chain-transfer agent grafted catheter prepared in step (2) was placed in the solution. The chain transfer agent (CTA) in solution phase prevents radical−radical coupling of surface polymer brush, resulting in a more uniform and well-controlled second block.[27] The solution was purged for 30 min with argon in a Schlenk tube. The polymerization was initiated by heating to 70 °C and carried out at this temperature for 12 h and then quenched in an ice-bath. The coated PU catheter was washed and sonicated in DI water to remove unattached homo poly(SBMA) and residual monomer. The terminal chain transfer agent was removed by heating the catheter in 10% butylamine in methanol solution at 40 °C for 1 h.

5.2.9. Surface Grafting of Nitric Oxide Release Precursor onto Catheter Coatings to Form (#8) H(N)-x-S, (#9) H(N)-r-S and (#10) H(N)-b-S. The synthesis of NO release precursor followed the scheme above (Scheme S1) as in section 5.2.5.2.

The surface grafted catheters ((#5) H-*r*-S, (#6) H-*x*-S, and (#7) H-*b*-S) were then added into prepared *S*-nitroso-3-mercapto-3-methylbutan-1-chloride (NTMB-Cl) solution (10 w/w% in hexane) and reacted with it for 12 h under an ice-bath. The modified catheters were washed in methanol and water for 4 h at 0 °C to remove unreacted NTMB-Cl. This produced catheters with NO emitting coatings ((#8) H(N)-*r*-S, (#9) H(N)-*x*-S, and (#10) H(N)-*b*-S).

5.2.10. Preparation of 30 cm-Long PU Catheter Coated with (#10) H(N)-b-S. A 30 cm PU catheter was cleaned using methanol and deionized water and subjected to the ozone treatment with ozone flowed through the bore at 0.6L/min for 30 min. The ozone-treated PU catheters were put under vacuum conditions (<10 Pa) at room temperature for 1 h to remove oxygen/ozone diffused into the PU. After activation, the catheter was connected to a peristaltic pump and put into a three-neck flask. The surface block copolymerization reactions and RSNO attachment like those in sections 5.2.8 and 5.2.9 were carried using this Plug-Flow reactor (Figure 1B) setup except the volumes of polymerization and RSNO attachment solutions were 100 mL. The reaction conditions such as argon purging, temperature, polymerization time, and concentrations of the monomer, thermal initiator, and chain transfer agent were same as section 5.2.8. The coating solution was circulated in the catheter at 10 mL/min. The surface grafting of the nitric oxide release precursor onto a longer (30 cm) PU catheter followed section 5.2.9.

5.2.11. Measurement of NO Release Precursor Leaching from Modified Catheter. The measurement of NO release precursor leaching from modified catheter followed ISO 10993-1 protocol; 5 mm pieces of modified catheters were extracted using PBS, polar solvent (methanol), and nonpolar solvent (Hexane). The extractants were analyzed using HPLC (Shimadzu LD-20) with UV detector (Shimadzu SPD-20) measuring absorbance at 341 nm (0.1 mg/mL of the NO release precursor, NTMB-Cl was used as standard).

5.2.12. Measurement of Nitric Oxide (NO) Release Profile from Modified Catheter ((#10) H(N)-b-S). 5 mm catheter samples were incubated in 1 mL of 10 mM PBS at pH 7.5 with 100 μM EDTA in darkness at 37 °C. Real-time release of NO into the solution was measured using a TBR 1025 free radical analyzer with a nitric oxide probe from World Precision Instruments.

For estimating the total RSNO concentration after grafting onto the polymer, the RSNO-catheter was heated to 55 °C and the NO-release flux was tracked until the NO release was complete. The amount of RSNO grafted was calculated as area under the NO-release flux curve.

https://dx.doi.org/10.1021/acscentsci.0c00755
ACS Cent. Sci. 2020, 6, 2031−2045

5.2.13. In vitro Catheter Antibacterial and Antibiofilm Efficacy Test. Microbe suspensions were prepared by scratching colonies from culture plates and inoculating them in protein rich medium (tryptic soy broth). The inoculums were incubated with shaking at 225 rpm at 37 °C to obtain overnight cultures. Catheter (5 mm long) samples including control sample were sterilized with 75% ethanol for 10 min at room temperature and then soaked in PBS overnight at 4 °C before testing.

5.2.13.1. Acute (2 h) Antibacterial Assay. The bacteria overnight cultures were washed thrice with PBS and resuspended in PBS at 10^8 CFU/mL. 10 μL of the suspension was spread onto each catheter piece. The catheter pieces were then incubated at 37 °C for 2 h with humidity not less than 90%. After the incubation, the catheter pieces were washed thoroughly using 100 μL of PBS to recover the microbes. CFU numbers were counted by serial dilution of the recovered bacteria suspensions and culture on lysogeny broth agar plates. All tests were performed one time with three independent biological replicates.

5.2.13.2. 24 h Biofilm Inhibition Test. Catheter pieces were immersed in 1 mL of TSB in a 24 well plate. 10^6 CFU/mL bacteria suspension in 10 mM PBS buffer was prepared by diluting the overnight inoculum. 8 μL of the PBS suspension of bacteria was added to each well. The catheter piece in TSB was then incubated for 24 h with orbital shaking at 110 rpm at 37 °C. After incubation, the catheter was removed from the inoculum and rinsed three times using PBS to remove planktonic bacteria. The catheter was then put in 1 mL of PBS buffer and sonicated for 15 min at 0 °C followed by 5 min vortex to recover the biofilm bacteria from the catheter surface. Bacterial suspension was serial diluted in PBS buffer and then grown on lysogeny broth (LB) agar plates at 37 °C overnight followed by CFU counting. All tests were performed one time with three independent biological replicates.

5.2.13.3. Long-Term Intraluminal Biofilm Inhibition Test (for 30 cm PU Catheter). The *in vitro* long-term intraluminal antibiofilm efficacy of long (30 cm) catheter was tested using a circulatory setup of physiological fluids.[11] The catheters were incubated in human serum for 30 min to mimic contact with blood. The catheter samples were then incubated in PBS suspension of bacteria, MRSA BAA38 or *P. aeruginosa*, with 10^8 CFU/mL for 2 h for initial attachment of bacteria which would form intraluminal biofilms. The catheter samples were then attached to a peristaltic pump which circulated brain heart infusion (BHI) medium maintained at 37 °C at 0.7 mL/min for defined study periods for biofilm growth. After the biofilm growth periods, the catheter samples were removed from the test apparatus and three pieces of 5 mm long catheters were cut from the initially 30 cm long catheter. The catheter was then placed in 1 mL of PBS buffer and sonicated for 15 min at 0 °C followed by 5 min of vortex to recover the biofilm bacteria from the catheter surface. Bacterial suspension was serial diluted in PBS buffer and then grown on lysogeny broth (LB) agar plates at 37 °C overnight followed by CFU counting. All tests were performed one time with three independent biological replicates.

For all *in vitro* catheter antibacterial and antibiofilm efficacy tests, the log reduction in microbe numbers of modified catheter compared with (#1) unmodified control catheter was calculated as

$$\log \text{reduction} = \log_{10}\left(\frac{\text{CFUs on (\#1) unmodified control}}{\text{CFUs on coated catheter}}\right)$$

5.2.14. In Vitro Biocompatibility Assay. 5.2.14.1. Cytotoxicity Assay. The cytotoxicity assay employed an extraction model adapted from ISO 10993-5 protocol.

3T3 fibroblasts, human embryonic kidney 293 cells (HEK), human dermal fibroblasts (HDF), and HepG2 cell lines obtained from ATCC were cultured in DMEM medium supplemented with 10% fetal bovine serum (FBS) and antibiotics (glutamine (2 mM), penicillin (100units/mL), and streptomycin (100 μg/mL)). The cells were maintained at 37 °C in a humidified incubator with 5% CO_2 until a monolayer, with greater than 80% confluence, was obtained.

Catheter pieces (5 mm long) were sterilized by soaking in ethanol/water (75/25) in 10 min at room temperature and then soaked in PBS overnight at 4 °C. Sterilized catheter pieces of 5 mm length were incubated in DMEM complete medium in sterile cell culture plates. The plates were incubated at 37 °C with 5% CO_2 in a humidified incubator for 24 h to extract soluble material from the catheter.

After 24 h-extraction, the cell line culture medium was discarded from the culture plates, and the cells were rinsed with PBS and the catheter extractants were added into the plate wells; the plates were then incubated for 24 h at 37 °C with 5% CO_2 in a humidified incubator. Then, 3-(4,5-dimethylthiazol-2-yl)-2,5-diphenyltetrazolium bromide, (MTT) (200 μL, 5 mg/mL) was added into each well, and the plates were incubated under the same condition for 4 h. The MTT was aspirated, and dimethyl sulfoxide (DMSO) was added into each well and the plates shaken (150 rpm) for 15 min. The absorbance of each well was measured at 570 nm using a microplate reader spectrophotometer (BIO-RAD, Benchmark Plus). All the assays were performed in three times with three independent biological replicates. The cell viability was calculated by the formula:

$$\%\ \text{cell viability} = \frac{\text{absorbance from cells incubated with catheter extractant}}{\text{absorbance from control cells incubated in pure DMEM}} \times 100\%$$

5.2.14.2. Activation of Immune Cells in Blood. Whole rabbit blood was used to test blood immunological response triggered by the catheters. The blood was freshly collected from the jugular vein of female New Zealand white rabbits by A*STAR and used immediately.

Sterilized 5 mm catheters were incubated with 100 μL of rabbit whole blood for 30 min. The blood was then fixed with 4% paraformaldehyde for 10 min at room temperature. The excess paraformaldehyde was then removed, and the cells were washed twice with PBS. Specific antibodies were dissolved in PBS and incubated with the blood samples for 1 h. (lymphocytes: CD3-APC and CD25-FTIC; monocytes: CD14-APC, CD11b-FTIC; platelets: CD41-FTIC, CD62p-APC; polymorphs: CD66b-APC, CD11-FTIC). The labeled blood cells were then washed twice with PBS to remove excess antibodies. Cell counts were performed using Attune NxT acoustic focusing cytometer. Blood without any treatment was used as negative control. The tests were performed one time with 3 independent biological replicates conducted.

5.2.14.3. Thrombus Activation and Formation Test. Whole rabbit blood was used to test blood immunological

https://dx.doi.org/10.1021/acscentsci.0c00755
ACS Cent. Sci. 2020, 6, 2031−2045

response triggered by the catheters. The blood was freshly collected from the jugular vein of female New Zealand white rabbits by A*STAR and used immediately.

Sterilized 5 mm catheters were incubated with 100 μL of rabbit whole blood for 2 h in a 96-well plate. The catheters were then washed with PBS thrice to remove unattached protein or blood cells. For quantification of thrombus formation by platelet aggregation test using adenosine diphosphate (ADP) assay: the catheter pieces were incubated with 100 μL of 5% disodium 4-nitrophenyl phosphate for 2 h. The catheters were removed and 100 μL of 1 M sodium hydroxide was added to the solution. The intensity of each well was measured with a plate reader under excitation wavelength of 405 nm. The test was performed one time with 3 independent biological replicates.

For scanning electronic microscopy observation of surface thrombi on catheter pieces, the blood incubated catheter pieces were washed with PBS thrice to remove unattached protein or blood cells and fixed with 4% paraformaldehyde in PBS solution overnight at 4 °C. The fixed catheter pieces were dehydrated in a graded ethanol series (25%, 50%, 75% and 100%). After dehydration, the ethanol was removed with an argon gas flow. The dried samples were imaged with a scanning electron microscope (JEOL JSM-6701F, Japan).

5.2.15. Surface Antifouling Test Using Blood Protein and Human Serum. Catheter pieces (5 mm long) were sterilized in 75% ethanol and soaked in PBS overnight before testing. The catheters were incubated with 1% fibrinogen, 10% albumin, or 50% human serum at 37 °C for 24 h. The catheters were then removed and washed thrice with PBS. The washed catheter samples were put in 1 mL of 1% SDS, shaken at 110 rpm for 2 h, and sonicated for 10 min. The catheters were removed, and the SDS solutions with protein detached from the catheters were incubated with bicinchoninic acid (BCA) protein assay kit solution for 30 min at 60 °C. The OD values of the SDS solutions were then measured at 562 nm. The protein concentrations were calculated according to the calibration curve provided in the kit.

5.2.16. In Vivo Murine and Porcine Models of Catheter-Associated Infections. In vivo murine subcutaneous implantation model:[28]

The experiments were performed according to the Institutional Animal Care and Usage Committee (IACUC) of the Nanyang Technological University (approved protocol number IACUC A18051, with approved amendment for subcutaneous catheter implantation). Overnight cultured bacteria were diluted in 1% TSB in PBS to give a final concentration of about 10^6 CFU/mL. Control and modified catheters were incubated with bacteria inoculum at 37 °C for 2 h. Seven to 9 weeks old female BALB/c mice were anesthetized by injection of Ketamine and shaved. 5 mm incisions were made on the backs of the mice. The bacteria-infected catheters were then inserted subcutaneously, and the incisions were then sealed with 3M Tegaderm. After 24 h, the mice were euthanized with CO_2. The implanted catheters were removed, and the condition of the lumens assessed. The samples were then sonicated to remove the adhered bacteria, which were serially diluted and plated on LB agar plates. CFU were counted after 24 h of incubation at 37 °C. The tests were performed one time with 5 independent biological replicates.

In vivo porcine hemodialysis catheterization model:[29]

The experiment was done in Beijing Maidisiwei Biotechnique service center with ethical protocol no. 202001094 approved by Northwestern Polytechnical University, China. Bama miniature pigs were utilized for porcine model studies. The recommended normal mean artery pressure (MAP) range is 84−107 mmHg, and the heart rate is 60−90 times per minute for Bama miniature pig.

5.2.16.1. Biocompatibility Test. The *in vivo* biocompatibility of modified catheter was proved by implantation in jugular vein of Pig (II) and in comparison with Pig (I) implanted with unmodified PU catheter as control. The jugular vein of only one side of Pig (I) or Pig (II) was implanted with one of the catheters. Bama miniature pig (50 kg) was anesthetized with an intramuscular injection of 4 mL of Zoletil-50 (25 mg/mL of zolazepam and 25 mg/mL of tiletamine) and 100 mg of xylazine. Inhalation of isoflurane (0.5−2% in pure oxygen) was maintained throughout the surgery. The pig was each placed in a supine position. The neck was shaved, and the skin of the surgical area was prepared with alcohol-based chlorhexidine and sterile dressings. The left jugular vein of the pig was exposed through standard open surgical techniques using a 5 cm skin incision. Before implantation, catheter was flushed and washed in sterile isotonic saline. The catheter was inserted by Seldinger technique. After insertion of the 10 cm-long catheter, the catheter was plugged. The wound and catheter were covered with sterile dressing. Butorphanol was used as painkiller with 3 doses per day. Biomarkers such as blood pressure, heart rate, breath rate, blood oxygen level were measured by a tail cuff and the skin temperature were monitored by infrared thermometer throughout 7 days of implantation. The test was performed one time with 1 independent biological replicate.

5.2.16.2. Antibiofilm Test with Introduction of Bacterial Infection. Bama miniature Pig III (50 kg) was anesthetized with an intramuscular injection of 4 mL of Zoletil-50 (25 mg/mL of zolazepam and 25 mg/mL of tiletamine) and 100 mg of xylazine. Inhalation of isoflurane (0.5−2% in pure oxygen) was maintained throughout the surgery. The pig was placed in a supine position. The neck was shaved, and the skin of the surgical area was prepared with alcohol-based chlorhexidine and sterile dressings. The bilateral jugular veins were exposed through standard open surgical techniques using a 5 cm skin incision. The unmodified catheter control (#1) and modified catheter (#10) were implanted in the left and right jugular veins respectively of the same pig for unbiased comparison. Before implantation, catheters were flushed and washed in sterile isotonic saline. The catheters were implanted in the jugular vein by Seldinger technique (unmodified catheter on left side and modified catheter on right side), the distal 10 cm of each catheter was immersed in a MRSA (BAA-40) suspension of 2×10^7 CFU/mL for 1 min and pushed completely into the jugular vein. The catheters were then plugged. The wounds and catheters were covered with sterile dressings. Biomarkers such as blood pressure, heart rate, breath rate, blood oxygen level were measured by tail cuff and skin temperature were monitored by infrared thermometer throughout implantation. No antibiotic was given before the surgery and during the experiment period. Butorphanol was used as pain killer with 3 doses per day. After 5 days, the pigs were euthanized, and the implanted catheters were removed and cut into pieces. Bacteria adhesion and thrombus formation on implanted catheters were observed by scanning electron microscopy, and bacteria adhesion on each piece of catheter

https://dx.doi.org/10.1021/acscentsci.0c00755
ACS Cent. Sci. 2020, 6, 2031−2045

was quantified by CFU counting. The test was performed one time with one independent biological replicate.

■ ASSOCIATED CONTENT

Supporting Information

The Supporting Information is available free of charge at https://pubs.acs.org/doi/10.1021/acscentsci.0c00755.

Synthesis and characterization details; quantification of NO-release precursors; stability test of coatings; SEM images; AFM images; other details (PDF)

■ AUTHOR INFORMATION

Corresponding Authors

Mary B. Chan-Park − *School of Chemical and Biomedical Engineering, Nanyang Technological University (NTU), Singapore 637459; Centre for Antimicrobial Bioengineering, NTU, Singapore 637459; School of Physical and Mathematical Sciences, Singapore 637371; Lee Kong Chian School of Medicine, Nanyang Technological University, Singapore 636921;* orcid.org/0000-0003-3761-7517; Email: mbechan@ntu.edu.sg

Peng Li − *Frontiers Science Center for Flexible Electronics (FSCFE), Xi'an Institute of Flexible Electronics (IFE) & Xi'an Institute of Biomedical Materials and Engineering (IBME), Northwestern Polytechnical University (NPU), Xi'an 710072, China;* orcid.org/0000-0002-5876-2177; Email: iampli@nwpu.edu.cn

Authors

Zheng Hou − *School of Chemical and Biomedical Engineering, Nanyang Technological University (NTU), Singapore 637459; Centre for Antimicrobial Bioengineering, NTU, Singapore 637459*

Yang Wu − *School of Chemical and Biomedical Engineering, Nanyang Technological University (NTU), Singapore 637459; Centre for Antimicrobial Bioengineering, NTU, Singapore 637459*

Chen Xu − *School of Chemical and Biomedical Engineering, Nanyang Technological University (NTU), Singapore 637459; Centre for Antimicrobial Bioengineering, NTU, Singapore 637459*

Sheethal Reghu − *School of Chemical and Biomedical Engineering, Nanyang Technological University (NTU), Singapore 637459; Centre for Antimicrobial Bioengineering, NTU, Singapore 637459;* orcid.org/0000-0001-5132-5196

Zifang Shang − *Frontiers Science Center for Flexible Electronics (FSCFE), Xi'an Institute of Flexible Electronics (IFE) & Xi'an Institute of Biomedical Materials and Engineering (IBME), Northwestern Polytechnical University (NPU), Xi'an 710072, China;* orcid.org/0000-0001-9062-0999

Jingjie Chen − *Frontiers Science Center for Flexible Electronics (FSCFE), Xi'an Institute of Flexible Electronics (IFE) & Xi'an Institute of Biomedical Materials and Engineering (IBME), Northwestern Polytechnical University (NPU), Xi'an 710072, China*

Dicky Pranantyo − *Department of Chemical & Biomolecular Engineering, National University of Singapore, Singapore 117585*

Kalisvar Marimuth − *Tan Tock Seng Hospital, Singapore 308433; Yong Loo Lin School of Medicine, National University of Singapore, Singapore 119228*

Partha Pratim De − *Tan Tock Seng Hospital, Singapore 308433*

Oon Tek Ng − *Lee Kong Chian School of Medicine, Nanyang Technological University, Singapore 636921; Tan Tock Seng Hospital, Singapore 308433; National Centre for Infectious Diseases, Singapore 308442*

Kevin Pethe − *Lee Kong Chian School of Medicine, Nanyang Technological University, Singapore 636921;* orcid.org/0000-0003-0916-8873

En-Tang Kang − *Department of Chemical & Biomolecular Engineering, National University of Singapore, Singapore 117585;* orcid.org/0000-0003-0599-7834

Complete contact information is available at: https://pubs.acs.org/10.1021/acscentsci.0c00755

■ ACKNOWLEDGMENTS

We thank the funding support from Singapore Ministry of Education Tier 3 grants (MOE2013-T3-1-002, MOE2018-T3-1-003), Singapore Ministry of Health Industry Alignment Fund (NMRC/MOHIAFCAT2/003/2014), as well as National Key R&D Program of China (2018YFC1105402). We also acknowledge the Centre Grant (CGAug16C005) and Clinician Scientist Award (MOH-000276). H.Z and W.Y acknowledge the support of NTU PhD scholarships.

■ REFERENCES

(1) George, J. Antibiotic-impregnated catheters for prevention of bloodstream infection. *Lancet* **2016**, *388* (10057), 2235.

(2) Costerton, J. W.; Stewart, P. S.; Greenberg, E. P. Bacterial Biofilms: A Common Cause of Persistent Infections. *Science* **1999**, *284* (5418), 1318.

(3) Weiner-Lastinger, L. M.; Abner, S.; Edwards, J. R.; Kallen, A. J.; Karlsson, M.; Magill, S. S.; Pollock, D.; See, I.; Soe, M. M.; Walters, M. S.; Dudeck, M. A.; et al. Antimicrobial-resistant pathogens associated with adult healthcare-associated infections: Summary of data reported to the National Healthcare Safety Network, 2015−2017. *Infection Control & Hospital Epidemiology* **2020**, *41* (1), 1.

(4) McGee, D. C.; Gould, M. K. Preventing Complications of Central Venous Catheterization. *N. Engl. J. Med.* **2003**, *348* (12), 1123.

(5) Casey, A. L; Mermel, L. A; Nightingale, P.; Elliott, T. S. Antimicrobial central venous catheters in adults: a systematic review and meta-analysis. *Lancet Infect. Dis.* **2008**, *8* (12), 763.

(6) Querido, M. M.; Aguiar, L.; Neves, P.; Pereira, C. C.; Teixeira, J. P. Self-disinfecting surfaces and infection control. *Colloids Surf., B* **2019**, *178*, 8.

(7) Haddadin, Y.; Annamaraju, P.; Regunath, H. *Central Line Associated Blood Stream Infections*. [Updated 2020 Aug 10]. Treasure Island (FL): StatPearls Publishing; **2020**. Available from: https://www.ncbi.nlm.nih.gov/books/NBK430891/.

(8) Geyer, F.; D'Acunzi, M.; Yang, C.-Y.; Muller, M.; Baumli, P.; Kaltbeitzel, A.; Mailander, V.; Encinas, N.; Vollmer, D.; Butt, H.-J. How to Coat the Inside of Narrow and Long Tubes with a Super-Liquid-Repellent Layer-A Promising Candidate for Antibacterial Catheters. *Adv. Mater.* **2019**, *31*, 1801324.

(9) Cloutier, M.; Mantovani, D.; Rosei, F. Antibacterial Coatings: Challenges, Perspectives, and Opportunities. *Trends Biotechnol.* **2015**, *33* (11), 637.

(10) Krishnamoorthy, M.; Hakobyan, S.; Ramstedt, M.; Gautrot, J. E. Surface-Initiated Polymer Brushes in the Biomedical Field: Applications in Membrane Science, Biosensing, Cell Culture, Regenerative Medicine and Antibacterial Coatings. *Chem. Rev.* **2014**, *114* (21), 10976.

(11) Smith, R. S.; Zhang, Z.; Bouchard, M.; Li, J.; Lapp, H. S.; Brotske, G. R.; Lucchino, D. L.; Weaver, D.; Roth, L. A.; Coury, A.; Biggerstaff, J.; Sukavaneshvar, S.; Langer, R.; Loose, C.; et al. Vascular Catheters with a Nonleaching Poly-Sulfobetaine Surface Modification Reduce Thrombus Formation and Microbial Attachment. *Sci. Transl. Med.* **2012**, *4* (153), No. 153ra132.
(12) Jain, G.; Allon, M.; Saddekni, S.; Barker, J.-F.; Maya, I. D. Does Heparin Coating Improve Patency or Reduce Infection of Tunneled Dialysis Catheters? *Clin. J. Am. Soc. Nephrol.* **2009**, *4* (11), 1787.
(13) Mi, L.; Jiang, S. Integrated Antimicrobial and Nonfouling Zwitterionic Polymers. *Angew. Chem., Int. Ed.* **2014**, *53* (7), 1746.
(14) Wang, W.; Lu, Y.; Xie, J.; Zhu, H.; Cao, Z. A zwitterionic macro-crosslinker for durable non-fouling coatings. *Chem. Commun.* **2016**, *52*, 4671.
(15) Roe, D.; Karandikar, B.; Bonn-Savage, N.; Gibbins, B.; Roullet, J.-B. Antimicrobial surface functionalization of plastic catheters by silver nanoparticles. *J. Antimicrob. Chemother.* **2008**, *61*, 869.
(16) Zhang, K.; Du, Y.; Si, Z.; Liu, Y.; Turvey, M. E.; Raju, C.; Keogh, D.; Ruan, L.; Jothy, S. L.; Reghu, S.; Marimuthu, K.; De, P. P.; Ng, O. T.; Mediavilla, J. R.; Kreiswirth, B. N.; Chi, Y. R.; Ren, J.; Tam, K. C.; Liu, X.-W.; Duan, H.; Zhu, Y.; Mu, Y.; Hammond, P. T.; Bazan, G. C.; Pethe, K.; Chan-Park, M. B. et al. Enantiomeric Glycosylated Cationic Block Co-Beta-Peptides Eradicate Staphylococcus Aureus Biofilms and Antibiotic-Tolerant Persisters. *Nat. Commun.* **2019**, *10*. DOI: 10.1038/s41467-019-12702-8
(17) Heard, S. O.; Wagle, M.; Vijayakumar, E.; McLean, S.; Brueggemann, A.; Napolitano, L. M.; Edwards, L. P.; O'Connell, F. M.; Puyana, J. C.; Doern, G. V. Influence of Triple Lumen Central Venous Catheters Coated With Chlorhexidine and Silver Sulfadizaine on the Incidence of Catheter-Related Bacteremia. *Arch. Intern. Med.* **1998**, *158* (1), 81.
(18) Yu, L.; Hu, P.; Chen, Y. Gas-Generating Nanoplatforms: Material Chemistry, Multifunctionality, and Gas Therapy. *Adv. Mater.* **2018**, *30*, 1801964.
(19) Hou, J.; Pan, Y.; Zhu, D.; Fan, Y.; Feng, G.; Wei, Y.; Wang, H.; Qin, K.; Zhao, T.; Yang, Q.; Zhu, Y.; Che, Y.; Liu, Y.; Cheng, J.; Kong, D.; Wang, P. G.; Shen, J.; Zhao, Q.; et al. Targeted delivery of nitric oxide via a 'bump-and-hole'-based enzyme−prodrug pair. *Nat. Chem. Biol.* **2019**, *15*, 151.
(20) Lutzke, A.; Tapia, J. B.; Neufeld, M. J.; Reynolds, M. M. Sustained Nitric Oxide Release from a Tertiary S-Nitrosothiol-based Polyphosphazene Coating. *ACS Appl. Mater. Interfaces* **2017**, *9* (3), 2104.
(21) Yang, T.; Zelikin, A. N.; Chandrawati, R. Progress and Promise of Nitric Oxide-Releasing Platforms. *Advanced Science* **2018**, *5*, 1701043.
(22) Ketchum, A. R.; Kappler, M. P.; Wu, J.; Xi, C.; Meyerhoff, M. E. The preparation and characterization of nitric oxide releasing silicone rubber materials impregnated with S-nitroso-tert-dodecyl mercaptan. *J. Mater. Chem. B* **2016**, *4*, 422.
(23) Terwel, D.; Nieland, L. J.M.; Schutte, B.; Reutelingsperger, C. P.M.; Ramaekers, F. C.S.; Steinbusch, H. W.M. S-nitroso-N-acetylpenicillamine and nitroprusside induce apoptosis in a neuronal cell line by the production of different reactive molecules. *Eur. J. Pharmacol.* **2000**, *400* (1), 19.
(24) Colletta, A.; Wu, J.; Wo, Y.; Kappler, M.; Chen, H.; Xi, C.; Meyerhoff, M. E. S-Nitroso-N-acetylpenicillamine (SNAP) Impregnated Silicone Foley Catheters: A Potential Biomaterial/Device To Prevent Catheter- Associated Urinary Tract Infections. *ACS Biomater. Sci. Eng.* **2015**, *1*, 416.
(25) Yu, W. H.; Kang, E. T.; Neoh, K. G. Controlled Grafting of Comb Copolymer Brushes on Poly(tetrafluoroethylene) Films by Surface-Initiated Living Radical Polymerizations. *Langmuir* **2005**, *21*, 450.
(26) Baum, M.; Brittain, W. J. Synthesis of Polymer Brushes on Silicate Substrates via Reversible Addition Fragmentation Chain Transfer Technique. *Macromolecules* **2002**, *35*, 610.
(27) Rowe-Konopacki, M. D.; Boyes, S. G. Synthesis of Surface Initiated Diblock Copolymer Brushes from Flat Silicon Substrates Utilizing the RAFT Polymerization Technique. *Macromolecules* **2007**, *40*, 879.
(28) Kadurugamuwa, J. L.; Sin, L.; Albert, E.; Yu, J.; Francis, K.; DeBoer, M.; Rubin, M.; Bellinger-Kawahara, C.; Parr, T. R.; Contag, P. R. Direct Continuous Method for Monitoring Biofilm Infection in a Mouse Model. *Infect. Immun.* **2003**, *71* (2), 882.
(29) Stenger, M.; Klein, K.; Grønnemose, R. B.; Klitgaard, J. K.; Kolmos, H. J.; Lindholt, J. S.; Alm, M.; Thomsen, P.; Andersen, T. E. Co-release of dicloxacillin and thioridazine from catheter material containing an interpenetrating polymer network for inhibiting device-associated Staphylococcus aureus infection. *J. Controlled Release* **2016**, *241*, 125.
(30) Raad, I.; Hanna, H.; Maki, D. Intravascular catheter-related infections: advances in diagnosis, prevention, and management. *Lancet Infect. Dis.* **2007**, *7*, 645.
(31) Munday, R. Toxicity of thiols and disulphides: Involvement of free-radical species. *Free Radical Biol. Med.* **1989**, *7* (6), 659.
(32) Munday, R. In vivo toxicity of thiols: Relationship to rate of one-electron oxidation by oxyhemoglobin. *Methods Enzymol.* **1995**, *251*, 117.
(33) Yang, X.; Chen, D.; Zhao, H. Silica particles with immobilized protein molecules and polymer brushes. *Acta Biomater.* **2016**, *29*, 446.
(34) Ryu, J. K.; Petersen, M. A.; Murray, S. G.; Baeten, K. M.; Meyer-Franke, A.; Chan, J. P.; Vagena, E.; Bedard, C.; Machado, M. R.; Coronado, P. E. R.; Prod'homme, T.; Charo, I. F.; Lassmann, H.; Degen, J. L.; Zamvil, S. S.; Akassoglou, K. et al. Blood coagulation protein fibrinogen promotes autoimmunity and demyelination via chemokine release and antigen presentation. *Nat. Commun.* **2015**, *6*. DOI: 10.1038/ncomms9164
(35) Fujimoto, K.; Takebayashi, Y.; Inoue, H.; Ikada, Y. Ozone-induced graft polymerization onto polymer surface. *J. Polym. Sci., Part A: Polym. Chem.* **1993**, *31* (4), 1035.
(36) Beija, M.; Marty, J.-D.; Destarac, M. RAFT/MADIX polymers for the preparation of polymer/inorganic nanohybrids. *Prog. Polym. Sci.* **2011**, *36*, 845.

https://dx.doi.org/10.1021/acscentsci.0c00755
ACS Cent. Sci. 2020, 6, 2031−2045